C.P. No. 428
(19,957)
A.R.C. Technical Report

C.P. No. 428
(19,957)
A.R.C. Technical Report

MINISTRY OF SUPPLY

AERONAUTICAL RESEARCH COUNCIL

CURRENT PAPERS

Some Simple Conical Camber Shapes to produce Low Lift-Dependent Drag on a Slender Delta Wing

by

G. G. Brebner

LONDON: HER MAJESTY'S STATIONERY OFFICE

1959

FOUR SHILLINGS NET

C.P. No. 428

U.D.C. No. 533.69.043.2

Technical Note No. Aero 2529

September, 1957

ROYAL AIRCRAFT ESTABLISHMENT

Some simple conical camber shapes to produce low lift-dependent drag on a slender delta wing

by

G. G. Brebner

SUMMARY

This note presents some of the theoretical aerodynamic characteristics of narrow delta wings having flat centre portions and two types of simple conical camber designed to produce zero load at the leading edge at the design C_L. Slender wing theory is used in the calculations. It is shown that the drag due to lift is comparable with the low values found by Smith and Mangler for wings with more "wavy" camber lines.

LIST OF CONTENTS

LIST OF ILLUSTRATIONS

1 Introduction

In a recent paper, Smith and Mangler[1] have described a method of designing conical camber distributions for thin triangular wings such that, at the design C_L, the load along the leading edge is zero. This condition on the load distribution was imposed in order to try to obtain a flow attachment line along the leading edge at the design C_L, even though the leading edge is sharp and highly swept. The lift-dependent drag would then be reduced compared with the plane wing with leading edge separation at the same C_L. The method was based on linearised supersonic theory, assuming conical flow, and the solutions included the "slenderness" parameter in a very convenient manner. Since the results for non-zero values of the slenderness parameter could be obtained from those with the slenderness parameter equal to zero (i.e. slender-wing theory), considerable attention was paid to the slender wing solution. In particular it was shown that for slender wings the camber could be designed to give lift-dependent drag factors as close to unity, the theoretical minimum for wings shedding substantially plane vortex sheets, as one wished. Thus a wing cambered to have an attachment line along the leading edge at its design C_L would be expected to show a useful reduction in lift-dependent drag compared with the corresponding sharp-edged uncambered wing having, at all non-zero lift coefficients, separation at the leading edge.

The camber shapes in the plane perpendicular to the line of flight obtained by Smith and Mangler[1] are wavy and contain a dihedral angle. The dihedral angle is not significant theoretically since an arbitrary additive function of y, the spanwise co-ordinate, is permitted, which could remove the dihedral. The waviness is due to the representation of the potential function by an infinite series. For calculation purposes, only the first N terms of the series are used and as N increases the lift-dependent drag factor decreases and the camber line contains more, but less pronounced, waves. To see whether comparable drag results could be obtained without waviness, it was thought worthwhile to examine the load distributions and lift-dependent drag characteristics of some slender delta wings with flat centre portions and simple conical camber shapes outboard, designed to have at the design C_L zero load at the leading edge. The wings were assumed to be flat over a triangular centre portion so that the downwash there was constant. Outboard of this region the downwash was assumed to vary in a simple conical manner. Using the relation between downwash and loading derived for slender wings in Ref.1 expressions were obtained in closed form for the load distributions and lift-dependent drag factors associated with two such downwash distributions, and the downwash itself was integrated to give the shape of the wing surface. The details of this calculation are given in section 2 and a discussion of the results in section 3.

It is known that, on a wing with conical geometry, deviations from conical flow are obtained in practice, especially near the trailing edge. Also, for practical applications slender wings with non-conical geometry may be preferable to deltas with conical camber. Nevertheless, the present results based on conical geometry and conical flow may prove useful in showing trends and defining downwash or load distributions for more general wing designs, as in a recent paper by Weber[2].

2 Theory

Let O, the origin of the co-ordinate system be at the apex of a slender delta wing. Ox is in the streamwise direction, Oy at right-angles to starboard and Oz at right-angles downwards. We assume that the angle of incidence and the camber are small enough for the boundary conditions on the wing (which is of zero thickness) to be applied in the

x,y plane, and for the trailing vortex sheet to lie in this plane. The root chord of the wing is taken as unity and the non-dimensional spanwise co-ordinate $\eta = y/Kx$ is used, where K is the semi-span at the trailing edge and Kx is the local semi-span s(x), (see Fig. 1). K is also the cotangent of the angle of sweep of the leading edge.

Equation (10) of Ref.1 gives the load in terms of the downwash on a slender wing, symmetrical about the x,z plane and having zero load at the leading edge, in conical flow:-

$$\frac{\ell(\eta)}{4K^2} = -\frac{1}{\pi}\int_{-1}^{1} \eta' \frac{d}{d\eta'}\left(\frac{w(\eta')}{KV}\right) \log\left|\frac{1 - \eta\eta' + \sqrt{\left(1-\eta^2\right)\left(1-\eta'^2\right)}}{\eta' - \eta}\right| d\eta'$$

allowing for the different sign convention in the z-direction. V is the free-stream velocity, $w(\eta)$ is the perturbation velocity in the z-direction, and $\ell(\eta) = {}^{-\Delta p}/_{\frac{1}{2}\rho V^2}$, the difference in pressure coefficient between the upper and lower surfaces. Since the flow is conical, w and ℓ are independent of x for a given η.

By reason of the symmetry of $w(\eta)$, the above equation may be written

$$\frac{\ell(\eta)}{4K^2} = -\frac{2}{\pi}\int_{0}^{1} \eta' \frac{d}{d\eta'}\left(\frac{w(\eta')}{KV}\right) \log \frac{\sqrt{1 - \eta'^2} + \sqrt{1 - \eta^2}}{\sqrt{\left|\eta'^2 - \eta^2\right|}}\, d\eta' \qquad (1)$$

There are an infinite number of downwash distributions $w(\eta')$, differing from each other by an additive constant, which have the same value of $\frac{dw}{d\eta'}$. Equation (1) gives the load distribution associated with that one member of this family for which the loading is zero at the leading edge. With any other additive constant, i.e. at any other incidence, $\ell(1) \neq 0$.

The lift-dependent drag coefficient is given by

$$C_{D_i} = \frac{1}{\bar{c}}\, 2 \int_{0}^{1} \ell(\eta)\, \frac{w(\eta)}{V}\, d\eta$$

where $\bar{c}$ is the mean chord. For a delta wing

$$C_{D_i} = \int_{0}^{1} \ell(\eta)\, \frac{w(\eta)}{V}\, d\eta \qquad (2)$$

and the lift-dependent drag factor, K_i, is

$$K_i = \frac{\pi A}{C_L^2} C_{D_i}$$

where A is the aspect ratio.

Since slender-wing theory is used, the wave drag due to lift is zero.

The shape of the surface relative to the leading edge is obtained from the stream surface condition.

$$\frac{\partial z}{\partial x} = \frac{w}{V}$$

$$z(x,y) - z_\ell(y) = \int_{x_\ell(y)}^{x} \frac{w}{V}\, dx \Big|_{y \text{ const.}}$$

$$= \frac{y}{K} \int_{\eta}^{1} \frac{w(\eta')}{V} \frac{d\eta'}{\eta'^2} \qquad (3)$$

where the suffix ℓ refers to the leading edge.

We shall start from downwash distributions of the general form

$$\left.\begin{aligned} \frac{w}{KV} &= a: && 0 \leqslant \eta \leqslant \overline{\eta} \\ \frac{w}{KV} &= a + b(\eta - \overline{\eta})^n: && \overline{\eta} < \eta \leqslant 1 \end{aligned}\right\}$$

where n is a positive integer. The case $n = 0$ has already been treated by Shaw[3] and is also discussed by Smith and Mangler[1]. The downwash is a step function and is associated with a plane delta wing having deflected leading edge flaps hinged about the line $\eta = \overline{\eta}$ = constant, the load along the hinge line being infinite. The cases treated in this note are $n = 1$ and 2.

2.1 Downwash distribution, $n = 1$

Consider a conical downwash distribution

$$\left.\begin{aligned} \frac{w(\eta)}{KV} &= a: && 0 \leqslant \eta \leqslant \overline{\eta} \\ \frac{w(\eta)}{KV} &= a + b(\eta - \overline{\eta}): && \overline{\eta} < \eta \leqslant 1 \end{aligned}\right\} \qquad (4)$$

Inboard of $\eta = \bar{\eta}$ the wing is flat and at a constant incidence $\alpha = Ka$. From equation (1),

$$\frac{\ell(\eta)}{4K^2} = -\frac{2b}{\pi}\int_{\bar{\eta}}^{1} \eta' \log \frac{\sqrt{1-\eta'^2}+\sqrt{1-\eta^2}}{\sqrt{|\eta'^2-\eta^2|}}\,d\eta'$$

$$= -\frac{b}{\pi}\left\{\left(\eta^2-\bar{\eta}^2\right)\log\frac{\sqrt{1-\bar{\eta}^2}+\sqrt{1-\eta^2}}{\sqrt{|\bar{\eta}^2-\eta^2|}}+\sqrt{1-\bar{\eta}^2}\,\sqrt{1-\eta^2}\right\} \quad (5)$$

When $\eta = \bar{\eta}$,

$$\frac{\ell(\bar{\eta})}{4K^2} = -\frac{b}{\pi}\lim_{\eta\to\bar{\eta}}\left\{\left(\eta^2-\bar{\eta}^2\right)\log\frac{\sqrt{1-\bar{\eta}^2}+\sqrt{1-\eta^2}}{\sqrt{|\bar{\eta}^2-\eta^2|}}+\sqrt{1-\bar{\eta}^2}\,\sqrt{1-\eta^2}\right\}$$

$$= -\frac{b}{\pi}\left(1-\bar{\eta}^2\right).$$

Equation (5), like equation (1), gives the load distribution associated with that member of the infinite family of downwash distributions (all of which have the same value of $\frac{dw}{d\eta}$) for which the loading at the leading edge is zero. This means that for a given value of b, $\ell(1) = 0$ only for one value of a, which is therefore dependent on b. To find the relation between them we substitute the expression for $\ell(\eta)/4K^2$ which has just been obtained (equation (5)) in the basic equation for the downwash, (equation (14) of Ref.1):-

$$\frac{w(\eta)}{KV} = -\frac{1}{\pi}\int_{-1}^{1}\frac{d}{d\eta'}\left(\frac{\ell(\eta')}{4K^2}\right)\log\frac{\sqrt{|\eta^2-\eta'^2|}}{|\eta|}\,\frac{d\eta'}{\eta'},$$

allowing for the different sign convention in the z-direction. Because of the symmetry of $w(\eta)$ and the relation

$$\int_{-1}^{1}\frac{d}{d\eta'}\left(\frac{\ell(\eta')}{4K^2}\right)\frac{d\eta'}{\eta'} = 0, \quad \text{(eqn. (8) of Ref.1)}$$

where the symbol $\oint$ means that the Cauchy Principal value has to be taken, we can write

$$\frac{w(\eta)}{KV} = -\frac{1}{\pi}\int_0^1 \frac{d}{d\eta'}\left(\frac{\ell(\eta')}{4K^2}\right)\log\left|\eta^2-\eta'^2\right|\frac{d\eta'}{\eta'} \qquad (6)$$

and identify this with (4). From (5) and (6),

$$\frac{w(\eta)}{KV} = \frac{b}{\pi^2}\int_0^1 \frac{d}{d\eta'}\left\{\left(\eta'^2-\bar{\eta}^2\right)\log\frac{\sqrt{1-\bar{\eta}^2}+\sqrt{1-\eta'^2}}{\sqrt{\left|\bar{\eta}^2-\eta'^2\right|}}+\sqrt{1-\bar{\eta}^2}\sqrt{1-\eta'^2}\right\}$$

$$\times\log\left|\eta^2-\eta'^2\right|\frac{d\eta'}{\eta'}$$

$$= \frac{2b}{\pi^2}\int_0^1 \left\{\log\frac{\sqrt{1-\bar{\eta}^2}+\sqrt{1-\eta'^2}}{\sqrt{\left|\bar{\eta}^2-\eta'^2\right|}}-\sqrt{\frac{1-\bar{\eta}^2}{1-\eta'^2}}\right\}\log\left|\eta^2-\eta'^2\right|d\eta'$$

Let $\eta = 0$.

$$\frac{w(0)}{KV} = \frac{4b}{\pi^2}\int_0^1 \left\{\log\frac{\sqrt{1-\bar{\eta}^2}+\sqrt{1-\eta'^2}}{\sqrt{\left|\bar{\eta}^2-\eta'^2\right|}}-\sqrt{\frac{1-\bar{\eta}^2}{1-\eta'^2}}\right\}\log\eta'\ d\eta'$$

$$= \frac{2b}{\pi}\left(\bar{\eta}\cos^{-1}\bar{\eta}-\sqrt{1-\bar{\eta}^2}\right)$$

$$= a \quad \text{on equating with the R.H.S. of (4).}$$

$$\therefore \frac{a}{b} = \frac{2}{\pi}\left(\bar{\eta}\cos^{-1}\bar{\eta}-\sqrt{1-\bar{\eta}^2}\right) \qquad (7)$$

At any fixed value of y, the chord load is given by

$$C_L(y)\ c(y) = \int_{x_\ell}^{1} \ell(\eta)\ dx \Big|_{y\ \text{const.}}$$

where $C_L(y)$ is the local lift coefficient,
$c(y)$ is the chord,

$$= \frac{y}{K} \int_{y/K}^{1} \ell(\eta)\ \frac{d\eta}{\eta^2}$$

Remembering that the root chord is unity, and writing $y/K = \eta_t$, the non-dimensional spanwise co-ordinate at the trailing edge, we have

$$C_L(\eta_t)\ c(\eta_t) = \frac{4bK^2}{\pi} \left\{ \left(\bar{\eta}^2 + \eta_t^2\right) \log \frac{\sqrt{1-\bar{\eta}^2} + \sqrt{1-\eta_t^2}}{\sqrt{|\bar{\eta}^2 - \eta_t^2|}} \right.$$

$$- \bar{\eta}\ \eta_t \log \frac{\bar{\eta}\sqrt{1-\eta_t^2} + \eta_t\sqrt{1-\bar{\eta}^2}}{\bar{\eta}\sqrt{1-\eta_t^2} - \eta_t\sqrt{1-\bar{\eta}^2}}$$

$$\left. - \sqrt{1-\bar{\eta}^2}\ \sqrt{1-\eta_t^2} \right\} \qquad (8)$$

When $\eta_t = \bar{\eta}$,

$$C_L(\bar{\eta})\ c(\bar{\eta}) = \frac{4bK^2}{\pi} \left\{ 2\bar{\eta}^2 \lim_{\eta_t \to \bar{\eta}} \log \frac{\sqrt{1-\bar{\eta}^2} + \sqrt{1-\eta_t^2}}{\sqrt{|\bar{\eta}^2 - \eta_t^2|}} \right.$$

$$\left. - 2\bar{\eta}^2 \lim_{\eta_t \to \bar{\eta}} \sqrt{\frac{\bar{\eta}\sqrt{1-\eta_t^2} + \eta_t\sqrt{1-\bar{\eta}^2}}{\bar{\eta}\sqrt{1-\eta_t^2} - \eta_t\sqrt{1-\bar{\eta}^2}}} - (1-\bar{\eta}^2) \right\}$$

$$= \frac{4bK^2}{\pi} \left\{ 2\bar{\eta}^2 \log \frac{1}{\bar{\eta}} - (1-\bar{\eta}^2) \right\} \qquad (9)$$

The total lift coefficient C_L is given by

$$C_L = \frac{1}{\bar{c}} \int_0^K C_L(y)\ c(y)\ dy \qquad \text{where } \bar{c} \text{ is the geometric mean chord}$$

$$= 2 \int_0^1 C_L(\eta_t)\ c(\eta_t)\ d\eta_t$$

$$= -\frac{4}{3} bK^2 \left(1 - \bar{\eta}^2\right)^{3/2} \tag{10}$$

and therefore

$$b = -\frac{3}{4} \frac{C_L}{K^2 (1 - \bar{\eta}^2)^{3/2}} \tag{11}$$

Alternatively C_L can be found directly from $\ell(\eta)$ which is constant along rays of constant η from the apex.

$$\therefore \quad C_L = 2 \int_0^1 \frac{1}{2} \ell(\eta)\ d\eta = -\frac{4}{3} bK^2 (1 - \bar{\eta}^2)^{3/2}$$

Equation (5) may now be rewritten

$$\frac{\ell(\eta)}{C_L} = \frac{3}{\pi (1 - \bar{\eta}^2)^{3/2}} \left\{ (\eta^2 - \bar{\eta}_1^2) \log \frac{\sqrt{1 - \bar{\eta}^2} + \sqrt{1 - \eta^2}}{\sqrt{|\bar{\eta}^2 - \eta^2|}} + \sqrt{1 - \bar{\eta}^2}\ \sqrt{1 - \eta^2} \right\} \tag{12}$$

and equation (8) becomes

$$\frac{C_L(\eta_t)\ c(\eta_t)}{C_L\ \bar{c}} = -\frac{6}{\pi\left(1-\bar{\eta}^2\right)^{3/2}}\left\{\left(\bar{\eta}^2+\eta_t^{\,2}\right)\log\frac{\sqrt{1-\bar{\eta}^2}+\sqrt{1-\eta_t^{\,2}}}{\sqrt{\left|\bar{\eta}^2-\eta^2\right|}}\right.$$

$$-\bar{\eta}\ \eta_t\ \log\frac{\bar{\eta}\sqrt{1-\eta_t^{\,2}}+\eta_t\sqrt{1-\bar{\eta}^2}}{\bar{\eta}\sqrt{1-\eta_t^{\,2}}-\eta_t\sqrt{1-\bar{\eta}^2}}$$

$$\left.-\sqrt{1-\bar{\eta}^2}\ \sqrt{1-\eta_t^{\,2}}\right\} \qquad (13)$$

From equations (4), (7) and (11) we get

$$\left.\begin{aligned}\frac{w(\eta)}{V}\ \frac{K}{C_L} &= -\frac{3}{2\pi}\ \frac{1}{\left(1-\bar{\eta}^2\right)^{3/2}}\left(\bar{\eta}\cos^{-1}\bar{\eta}-\sqrt{1-\bar{\eta}^2}\right) : 0 \leq \eta \leq \bar{\eta}\\ &= -\frac{3}{4}\ \frac{1}{\left(1-\bar{\eta}^2\right)^{3/2}}\\ &\quad\times\left\{\frac{2}{\pi}\left(\bar{\eta}\cos^{-1}\bar{\eta}-\sqrt{1-\bar{\eta}^2}\right)+(\eta-\bar{\eta})\right\} : \quad \bar{\eta} < \eta \leq 1\end{aligned}\right\} \qquad (14)$$

From equation (2) the lift-dependent drag is

/equation (15)

$$C_{D_i} = -\frac{C_L^2}{\pi K}\,\frac{9}{4(1-\bar{\eta}^2)^3}\left[\int_0^1\left\{\left(\eta^2-\bar{\eta}^2\right)\log\frac{\sqrt{1-\bar{\eta}^2}+\sqrt{1-\eta^2}}{\sqrt{|\,\bar{\eta}^2-\eta^2|}}+\sqrt{1-\bar{\eta}^2}\,\sqrt{1-\eta^2}\right\}\right.$$

$$\times\ \frac{2}{\pi}\left(\bar{\eta}\cos^{-1}\bar{\eta}-\sqrt{1-\bar{\eta}^2}\right)\ d\eta$$

$$\left.+\int_{\bar{\eta}}^1\left\{\left(\eta^2-\bar{\eta}^2\right)\log\frac{\sqrt{1-\bar{\eta}^2}+\sqrt{1-\eta^2}}{\sqrt{|\,\bar{\eta}^2-\eta^2\,|}}+\sqrt{1-\bar{\eta}^2}\,\sqrt{1-\eta^2}\right\}(\eta-\bar{\eta})\ d\eta\right] \qquad (15)$$

and the induced drag factor is

$$K_i = C_{D_i}\frac{\pi A}{C_L^2} = C_{D_i}\frac{4\pi K}{C_L^2}$$

$$= -\frac{3}{2(1-\bar{\eta}^2)^3}\left[4\left\{\bar{\eta}^4\log\bar{\eta}-(1-\bar{\eta}^2)^2\right\}+(3-\bar{\eta}^2)(1-\bar{\eta}^2)\right] \qquad (16)$$

Finally, the shape of the surface (relative to its leading edge) associated with the given downwash distribution is found from equation (3):-

$$z(x,y) - z_{\ell}(y) = \int_{x_{\ell}(y)}^{x}\frac{w}{V}\,dx\,\Big|_{y\ \text{const.}}$$

Let $\bar{x} \leqslant x \leqslant 1$ so that $0 \leqslant \eta \leqslant \bar{\eta}$ $\left(\bar{x} = \bar{x}(y) = \frac{y}{K\bar{\eta}}\right)$

Then

$$z(x,y) - z_\ell(y) = \int_{x_\ell}^{\bar{x}} K\left\{a + b(\eta - \bar{\eta})\right\} dx + \int_{\bar{x}}^{x} Ka \quad dx$$

$$= \int_{x_\ell}^{x} Ka \quad dx + \int_{\bar{\eta}}^{1} Kb(\eta - \bar{\eta}) \quad \frac{y}{K} \quad \frac{d\eta}{\eta^2}$$

$$= Ka\left(x - \frac{y}{K}\right) + Kb\,\frac{y}{K}\left(\bar{\eta} - 1 - \log \bar{\eta}\right)$$

since $x_\ell = \frac{y}{K}$.

$Ka = \alpha$, the incidence of the centre part of the wing, $0 \leqslant \eta \leqslant \bar{\eta}$, which is defined to be flat and at constant incidence. Therefore in this region

$$\frac{\partial z}{\partial x} = \alpha : \quad z(x) = \alpha x = Ka\,x.$$

and therefore

$$z_\ell = K\,\frac{y}{K}\left\{a - b\left(\bar{\eta} - 1 - \log \bar{\eta}\right)\right\}$$

Let $x_\ell \leqslant x < \bar{x}$ so that $\bar{\eta} < \eta \leqslant 1$.

Then

$$z(x,y) - z_\ell(y) = \int_{x_\ell}^{x} K\left\{a + b(\eta - \bar{\eta})\right\} dx$$

$$= Ka\left(x - \frac{y}{K}\right) + Kb\,\frac{y}{K}\left(\bar{\eta} - \frac{\bar{\eta}}{\eta} - \log \eta\right)$$

$$\therefore \quad z(x) = K\left\{ax + b\,\frac{y}{K}\left(1 - \frac{\bar{\eta}}{\eta} + \log \frac{\bar{\eta}}{\eta}\right)\right\}$$

$$= Kx\left\{a + b\left(\eta - \bar{\eta} + \eta \log \frac{\bar{\eta}}{\eta}\right)\right\} \quad \text{since } \frac{y}{K} = \eta x.$$

In terms of the local semispan, $s(x) = Kx$,

$$\left.\begin{aligned} \frac{z(x,y)}{s(x)} = \frac{z}{s}(\eta) &= a; && 0 \leqslant \eta \leqslant \bar{\eta} \\ &= a + b(\eta - \bar{\eta} + \eta \log \frac{\bar{\eta}}{\eta}); && \bar{\eta} < \eta \leqslant 1 \end{aligned}\right\}$$

i.e.

$$\left.\begin{aligned} \frac{z}{s}(\eta)\ \frac{K^2}{C_L} &= -\frac{3}{2\pi\,(1-\bar{\eta}^{-2})^{3/2}}\left(\bar{\eta}\cos^{-1}\bar{\eta} - \sqrt{1-\bar{\eta}^{2}}\right); && 0 \leqslant \eta \leqslant \bar{\eta} \\ &= -\frac{3}{4\,(1-\bar{\eta}^{2})^{3/2}}\left\{\frac{2}{\pi}\left(\bar{\eta}\cos^{-1}\bar{\eta} - \sqrt{1-\eta^{-2}}\right)\right. \\ &\qquad \left. + \eta - \bar{\eta} + \eta \log \frac{\bar{\eta}}{\eta}\right\}; && \bar{\eta} < \eta \leqslant 1 \end{aligned}\right\} \quad (17)$$

2.2 Downwash distribution, n = 2

As in section 2.1 we consider a downwash distribution which is constant for $0 \leqslant \eta \leqslant \bar{\eta}$:-

$$\left.\begin{aligned} \frac{w(\eta)}{V} &= a; && 0 \leqslant \eta \leqslant \bar{\eta} \\ \frac{w(\eta)}{V} &= a + b(\eta - \bar{\eta})^{2}; && \bar{\eta} < \eta \leqslant 1 \end{aligned}\right\} \quad (18)$$

The aerodynamic properties and geometric characteristics associated with this downwash are obtained as in section 2.1 and are given by the following equations:-

$$\frac{\ell(\eta)}{C_L} = \frac{8}{\pi\left\{3\cos^{-1}\bar{\eta} - \bar{\eta}\sqrt{1-\bar{\eta}^{-2}}\left(5-2\bar{\eta}^{-2}\right)\right\}}\left[\bar{\eta}\left(\bar{\eta}^{-2}-3\eta^{2}\right)\log\frac{\sqrt{1-\bar{\eta}^{-2}}+\sqrt{1-\eta^{2}}}{\sqrt{|\bar{\eta}^{-2}-\eta^{2}|}}\right.$$

$$+ \eta^{3}\log\frac{\bar{\eta}\sqrt{1-\eta^{2}}+\eta\sqrt{1-\bar{\eta}^{-2}}}{\bar{\eta}\sqrt{1-\eta^{2}}-\eta\sqrt{1-\bar{\eta}^{-2}}}$$

$$\left. + \sqrt{1-\eta^{2}}\left\{\left(1+2\eta^{2}\right)\cos^{-1}\bar{\eta} - 2\bar{\eta}\sqrt{1-\bar{\eta}^{-2}}\right\}\right] \quad \ldots (19)$$

When $\eta = \bar{\eta}$,

$$\frac{\ell(\bar{\eta})}{C_L} = \frac{8}{\pi\left\{3\cos^{-1}\bar{\eta} - \bar{\eta}\sqrt{1-\bar{\eta}^2}\left(5-2\bar{\eta}^2\right)\right\}} \times$$

$$\times\left[2\bar{\eta}^3 \log \bar{\eta} + \sqrt{1-\bar{\eta}^2}\left\{\left(1+2\bar{\eta}^2\right)\cos^{-1}\bar{\eta} - 2\bar{\eta}\sqrt{1-\bar{\eta}^2}\right\}\right]$$

$$\frac{C_L(\eta_t)\, c(\eta_t)}{C_L\, \bar{c}} = \frac{8}{\pi\left\{3\cos^{-1}\bar{\eta} - \bar{\eta}\sqrt{1-\bar{\eta}^2}\left(5-2\bar{\eta}^2\right)\right\}} \times$$

$$\times\left[-\bar{\eta}\left(\bar{\eta}^2+3\eta_t^{\,2}\right)\log\frac{\sqrt{1-\bar{\eta}^2}+\sqrt{1-\eta_t^{\,2}}}{\sqrt{\left|\bar{\eta}^2-\eta_t^{\,2}\right|}}\right.$$

$$+\eta_t\frac{3\bar{\eta}^2+\eta_t^{\,2}}{2}\log\frac{\bar{\eta}\sqrt{1-\eta_t^{\,2}}+\eta_t\sqrt{1-\bar{\eta}^2}}{\bar{\eta}\sqrt{1-\eta_t^{\,2}}-\eta_t\sqrt{1-\bar{\eta}^2}}$$

$$\left.-\sqrt{1-\eta_t^{\,2}}\left\{\left(1-\eta_t^{\,2}\right)\cos^{-1}\bar{\eta} - 2\bar{\eta}\sqrt{1-\bar{\eta}^2}\right\}\right] \qquad (20)$$

$$\left.\begin{aligned}\frac{w(\eta)}{V}\,\frac{K}{C_L} &= -\frac{3}{\pi}\,\frac{3\bar{\eta}\sqrt{1-\bar{\eta}^2}-\left(1+2\bar{\eta}^2\right)\cos^{-1}\bar{\eta}}{3\cos^{-1}\bar{\eta}-\bar{\eta}\sqrt{1-\bar{\eta}^2}\left(5-2\bar{\eta}^2\right)}\ ;\ 0\le\eta\le\bar{\eta}\\ &= -\frac{3}{3\cos^{-1}\bar{\eta}-\bar{\eta}\sqrt{1-\bar{\eta}^2}\left(5-2\bar{\eta}^2\right)}\times\\ &\quad\times\left\{\frac{3\bar{\eta}\sqrt{1-\bar{\eta}^2}-\left(1+2\bar{\eta}^2\right)\cos^{-1}\bar{\eta}}{\pi}+(\eta-\bar{\eta})^2\right\}\ ;\ \bar{\eta}<\eta\le 1\end{aligned}\right\} \quad \ldots\ (21)$$

$$K_i = C_{D_i} \frac{4\pi K}{C_L^2}$$

$$= -\frac{4}{5\left\{3\cos^{-1}\bar{\eta} - \bar{\eta}\sqrt{1-\bar{\eta}^2}\left(5-2\bar{\eta}^2\right)\right\}^2} \times$$

$$\times \left\{ \begin{array}{l} 64\bar{\eta}^6 \log \bar{\eta} + \bar{\eta}\sqrt{1-\bar{\eta}^2}\cdot\cos^{-1}\bar{\eta}\cdot\left(54-28\bar{\eta}^2+4\bar{\eta}^4\right) \\ -\bar{\eta}^2\left(1-\bar{\eta}^2\right)\left(51-68\bar{\eta}^2\right) - 15\left(\cos^{-1}\bar{\eta}\right)^2 \end{array} \right\} \qquad (22)$$

and finally,

$$\left.\begin{aligned} \frac{z}{s}(\eta)\cdot\frac{K^2}{C_L} &= -\frac{3}{\pi}\cdot\frac{3\bar{\eta}\sqrt{1-\eta^2} - \left(1+2\bar{\eta}^2\right)\cos^{-1}\bar{\eta}}{3\cos^{-1}\bar{\eta} - \bar{\eta}\sqrt{1-\bar{\eta}^2}\left(5-2\bar{\eta}^2\right)}; \quad 0 \le \eta < \bar{\eta} \\ &= -\frac{3}{3\cos^{-1}\bar{\eta} - \bar{\eta}\sqrt{1-\bar{\eta}^2}\left(5-2\bar{\eta}^2\right)} \times \\ &\times \left\{\frac{3\eta\sqrt{1-\bar{\eta}^2} - \left(1+2\bar{\eta}^2\right)\cos^{-1}\bar{\eta}}{\pi} + \bar{\eta}^2 - \eta^2 - 2\eta\bar{\eta}\log\frac{\bar{\eta}}{\eta}\right\}; \\ &\qquad \bar{\eta} < \eta \le 1 \end{aligned}\right\} \qquad (23)$$

3 Discussion of results

Figs. 2-12 illustrate the downwash and load distributions, cross-section shape, spanwise distribution of chord load and lift-dependent drag factor for the two types of camber considered. The results have been calculated for $\bar{\eta} > 0.6$ only, as K_i increases with decreasing $\bar{\eta}$ and $\bar{\eta} < 0.6$ may not be of much practical interest.

Figs. 3 and 5 show the effect of n on the cross-section shapes. When $n = 0$ (leading edge flaps deflected for zero load at the leading edge) the slope $\frac{d}{d\eta}\left(\frac{z}{s}\right)$ is discontinuous at $\eta = \bar{\eta}$. When $n = 1$, Fig. 3 shows that the slope is continuous but the maximum curvature is still quite pronounced close to $\eta = \bar{\eta}$. Such a sharp curvature is probably not a good feature as it may give rise to a separation, even though the flow is

attached at the leading edge. It may be noted that for $n = 1$ the section shape outboard of $\eta = \bar{\eta}$ is very nearly a parabola. Fig. 5 shows that when $n = 2$ the maximum curvature is less pronounced and has moved towards the tip.

Since the camber and incidence are proportional to the design C_L, the latter should be such that the camber and incidence are small enough to justify the use of linearised theory.

The surface slope at the leading edge is of interest since it may influence the leading edge separation characteristics at off-design lift coefficients. One feels that for this reason, as well as to comply with the assumptions of the linearised theory regarding the related quantity $\frac{\partial z}{\partial x}$, this slope should be kept as small as possible. Fig. 6 shows $\left[\frac{d}{d\eta}\left(\frac{z}{s}\right)\right]_{\eta=1}$ plotted against $\bar{\eta}$ for $n = 1$ and 2. It is interesting to note that the slope is a minimum for $\bar{\eta} = 0.68$ when $n = 1$ and for $\bar{\eta} = 0.67$ when $n = 2$. For equal values of $\bar{\eta}$ the slope at the leading edge is always greater for $n = 2$ than for $n = 1$.

The load distributions in planes perpendicular to the stream direction are saddle-shaped (Figs. 7 and 8), the peaks occurring outboard of $\eta = \bar{\eta}$. The peaks are finite, however, in contrast to the plane wing at incidence or the wing with leading edge flaps deflected for zero load at the leading edge, which have theoretically infinite suctions at the leading edge and the hinge line respectively. Figs. 9 and 10 show the spanwise distribution of chord load and it can be seen that this becomes more nearly elliptic as $\bar{\eta} \to 1$. When $\bar{\eta} = 1$ the design condition of zero load at the leading edge cannot be realised. The wing cross-section shape degenerates into a plane wing at incidence. The load at the leading edge is infinite, except in the trivial case when the design C_L is zero, i.e. the incidence is zero. Because of the delta planform, the spanwise distribution of chord load can only be elliptic if the loading at the leading edge is infinite, and so it can never be achieved with a wing designed for zero loading at $\eta = 1$. In fact the slope of the chord load distribution, $\frac{d}{dy}\frac{C_L(y)\ c(y)}{C_L\ \bar{c}}$ is zero at the tip, $\eta_t = y/K = 1.0$, and not infinite as would be required for elliptic loading.

The lift-dependent drag factor, K_i, depends on the shape of the spanwise distribution of chord load. When this is elliptic the theoretical minimum value $K_i = 1.0$ is obtained for a wing with a plane vortex sheet springing from the trailing edge and no wave drag. Thus $K_i = 1.0$ only for the plane wing with infinite loading at the leading edge. The purpose of the present work is to see how small K_i can be for slender delta wings with simple camber distributions to give zero load at the leading edge. The variation of K_i with $\bar{\eta}$ is shown in Fig. 11 for $n = 0$, 1 and 2. In all cases K_i decreases almost linearly to its minimum value of unity between $\bar{\eta} = 0.6$ and $\bar{\eta} = 1.0$. For a given $\bar{\eta}$, K_i decreases as n increases but the rate of decrease falls off rapidly and no substantial improvement is likely to be obtained for $n > 2$. For a given K_i, $\bar{\eta}$ decreases as n increases, i.e. a greater proportion of the wing area must

be cambered. Referring back to Fig. 6 we see that for a given K_i (in this case $K_i = 1.05$) the surface slope $\frac{d}{d\eta}\left(\frac{z}{s}\right)$ at the leading edge increases with n.

Fig. 11 also contains the lift-dependent drag factors calculated by Smith and Mangler[1]. N is the number of terms retained in their infinite series for K_i, and the latter decreases as N increases. At the same time however the number of "waves" in their cross-section shape increases, although their amplitude becomes smaller, and the shape becomes less suitable for practical application. Fig. 11 shows that values of K_i comparable with the lowest values quoted by Smith and Mangler can be obtained by the simpler shapes of wing cross-section developed in section 2.

In principle any reasonable value of $K_i > 1.0$ can be obtained with any value of n by choosing the appropriate $\bar{\eta}$. In practice the particular wing shape chosen will depend on a number of requirements, some of which are conflicting. For example, Fig. 12 shows the spanwise load distribution at any cross-section for wings having approximately the same K_i ($K_i = 1.05$, $n = 1$ and 2, and $K_i = 1.035$, $n = 0$). For $n = 0$ there is of course an infinite suction at the hinge line. As n increases the peak suction decreases but there is not much difference in this respect between $n = 1$ and $n = 2$, and elsewhere the load distributions are almost identical. To avoid flow separation occurring on the upper surface of the wing, low suction peaks and an absence of sharp changes of curvature are desirable and this implies large n. On the other hand for a low value of the cross-section slope at the leading edge, n should be small, and $\bar{\eta}$ in the neighbourhood of 0.67. Again, a large area of plane wing might be welcome for structural simplicity, which implies large $\bar{\eta}$ and small n. However, for the off-design condition with flow separation from the leading edge, it might be desirable to have a fairly large area of forward-facing surface outboard of $\bar{\eta}$, so that the high suctions under the rolled-up vortex sheets would give rise to a force component tending to reduce the drag. This would imply small $\bar{\eta}$ and large n. The choice of a wing shape therefore involves a compromise between various factors.

The characteristics of wing shapes with $n > 2$ have not been calculated as the marginal improvements in K_i did not seem to be worth the increasing mathematical complexity. Wing shapes given by $n = 1$ and $n = 2$ seem likely to meet most practical requirements.

NOTATION

x,y,z	Rectangular co-ordinates, origin at apex of wing, non-dimensional in terms of root chord: z positive downwards.
K	Cotangent of angle of sweep of leading edge = semi-span of wing.
$s(x)$	Local semi-span.
η	Non-dimensional spanwise co-ordinate = $y/s(x)$.
η_t	y/K.
$\bar{\eta}$	Ray from apex outboard of which the surface is cambered.

NOTATION (Contd)

V	Free-stream velocity.
w	Perturbation velocity in z-direction.
Δp	Difference between pressures on upper and lower surfaces.
ℓ	local non-dimensional load $= -\Delta p / \frac{1}{2}\rho V^2$.
$c(y)$	local chord.
$\bar{c}$	Geometric mean chord.
$C_L(y)$	Local lift coefficient.
C_L	Overall lift coefficient.
C_{D_i}	Lift-dependent drag coefficient.
K_i	Lift-dependent drag factor, $= C_{D_i} \frac{\pi A}{C_L^2}$.
A	Aspect Ratio.
α	angle of incidence.
a, b, n	Parameters in downwash distribution.

REFERENCES

No.	Author	Title, etc.
1	J.H.B. Smith and K.W. Mangler	The use of conical camber to produce flow attachment at the leading edge of a delta wing and to minimise lift-dependent drag at sonic and supersonic speeds. R.A.E. Report No. Aero 2584, 1957. A.R.C. 19,961
2	J. Weber	Design of warped slender wings with the attachment line along the leading edge. R.A.E. Tech. Note to be issued.
3	B.W.B. Shaw	Nose controls on delta wings at supersonic speeds. College of Aeronautics, Cranfield, Rep. No. 36, May 1950: A.R.C. 13,372.

WT.2078.C.P.428.K3 - Printed in Great Britain

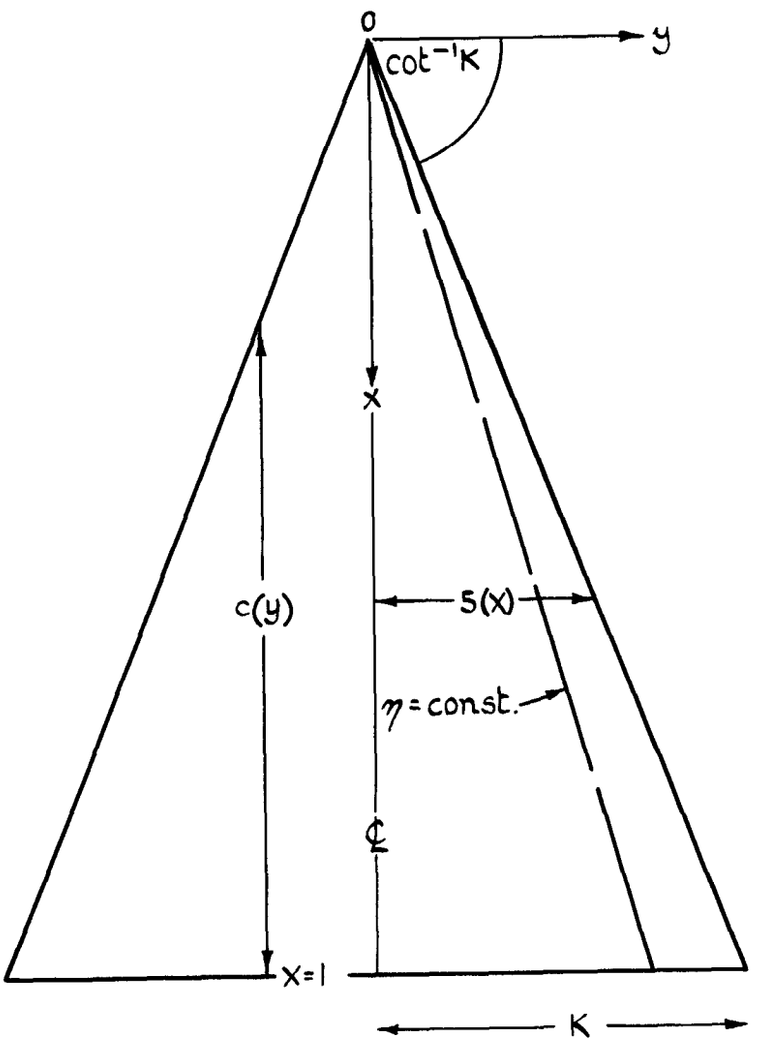

FIG.1. NOTATION.

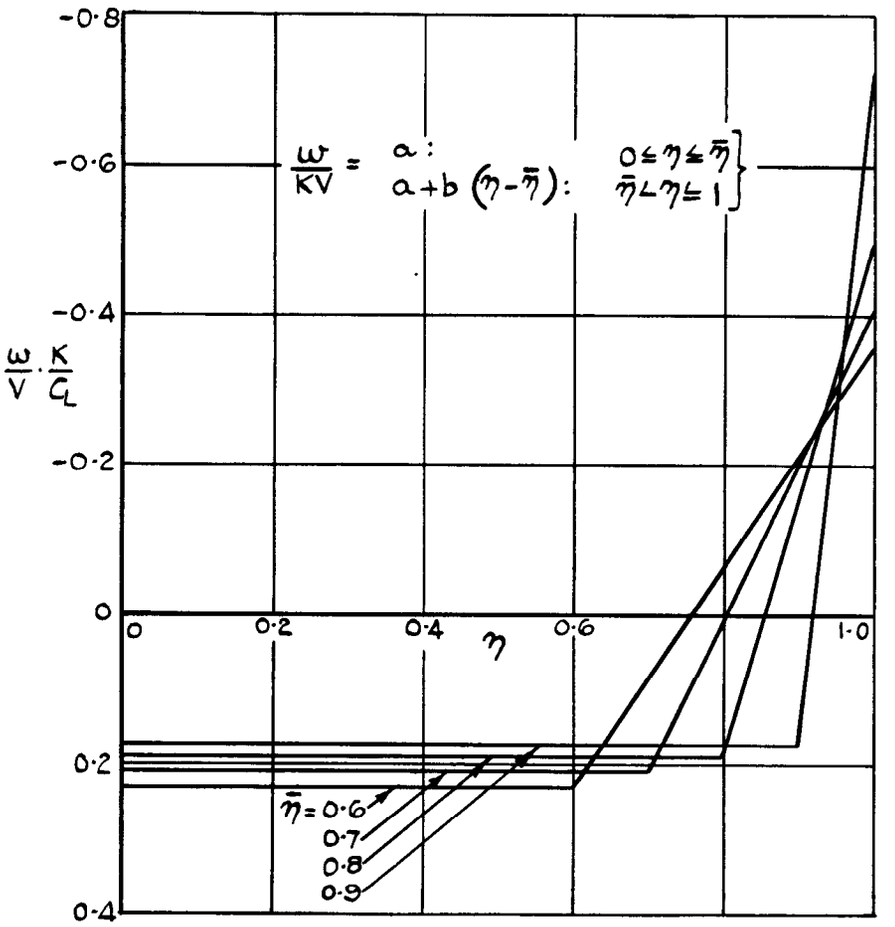

FIG.2. SPANWISE DOWNWASH DISTRIBUTION: $n = 1$.

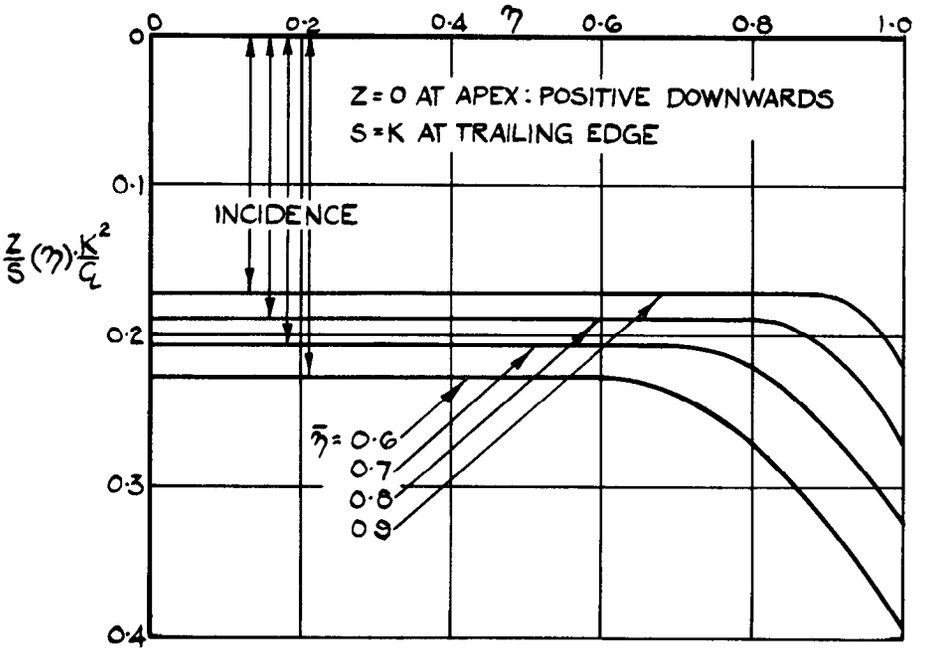

FIG.3. CROSS-SECTION SHAPE (THIN WING) $n = 1$.

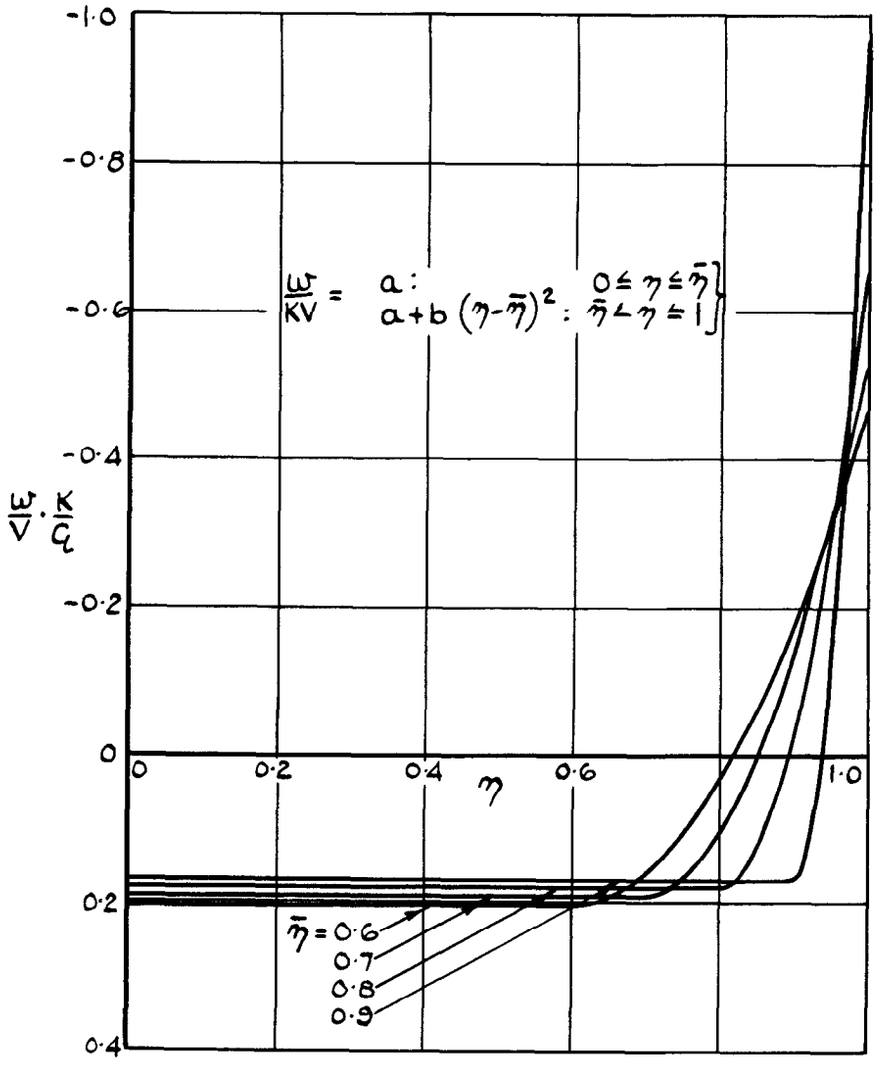

FIG. 4. SPANWISE DOWNWASH DISTRIBUTION

$n = 2$

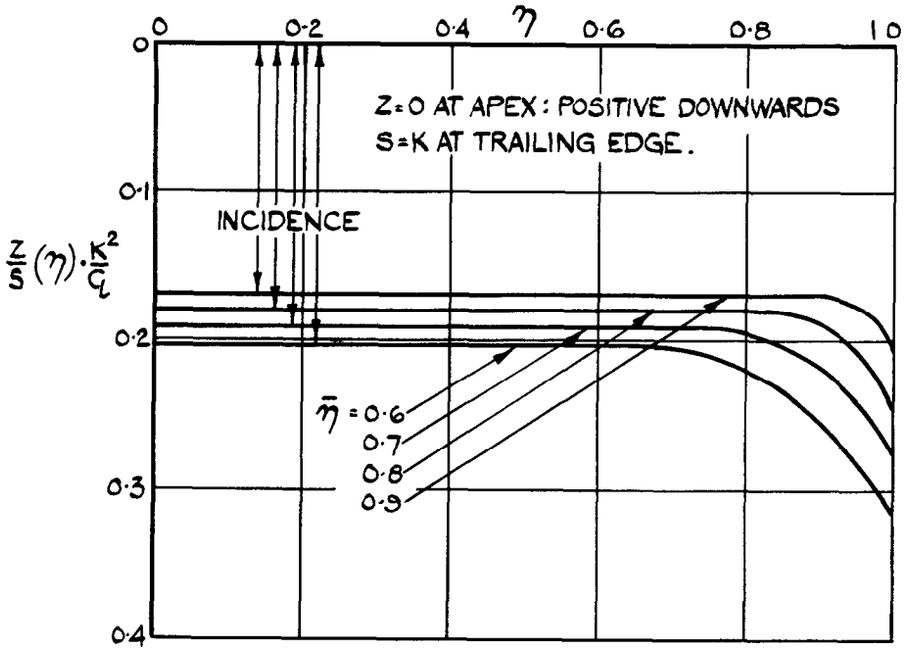

FIG. 5. CROSS-SECTION SHAPE (THIN WING)

$n = 2$

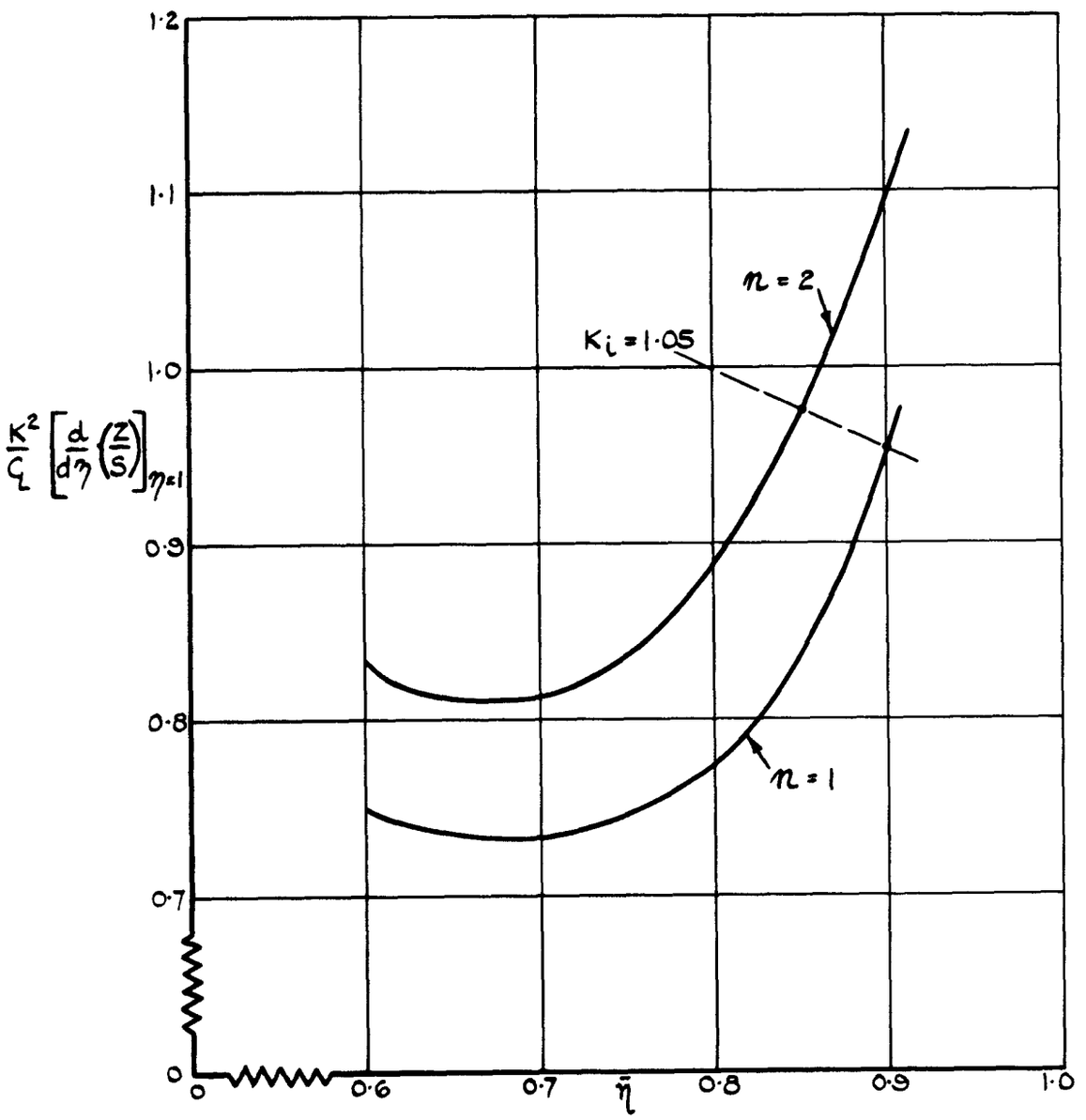

FIG. 6. SURFACE SLOPE, $\frac{d}{d\eta}\left(\frac{Z}{S}\right)$, AT LEADING EDGE.

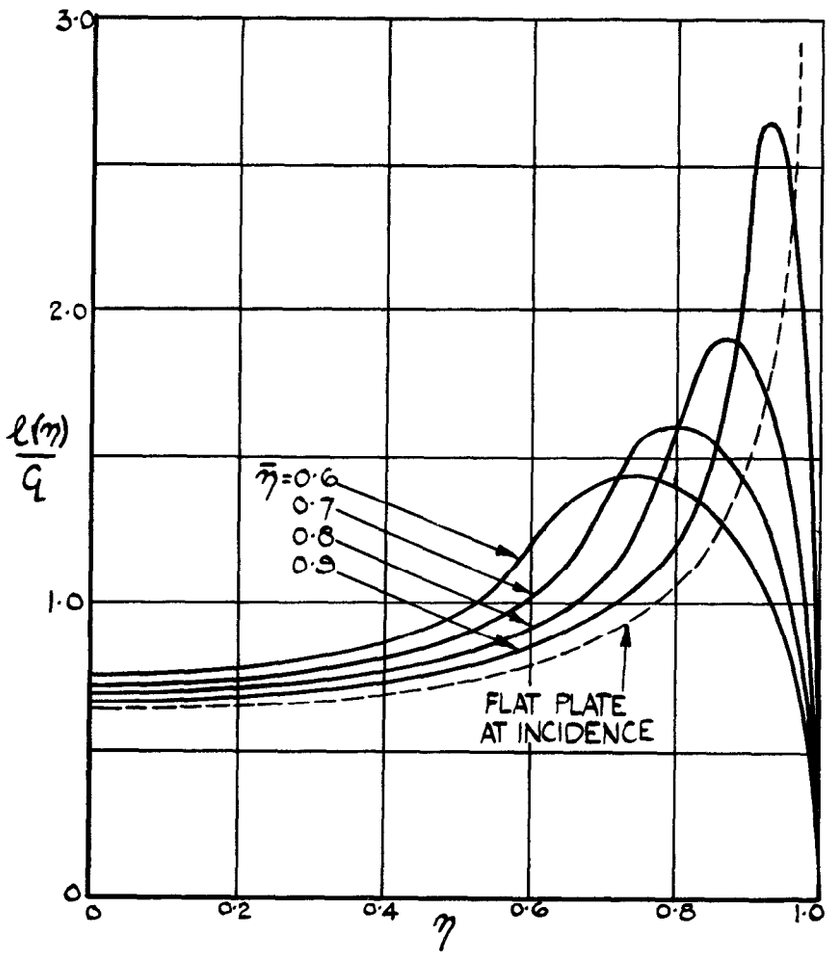

FIG.7. SPANWISE LOAD DISTRIBUTION.
$n = 1$.

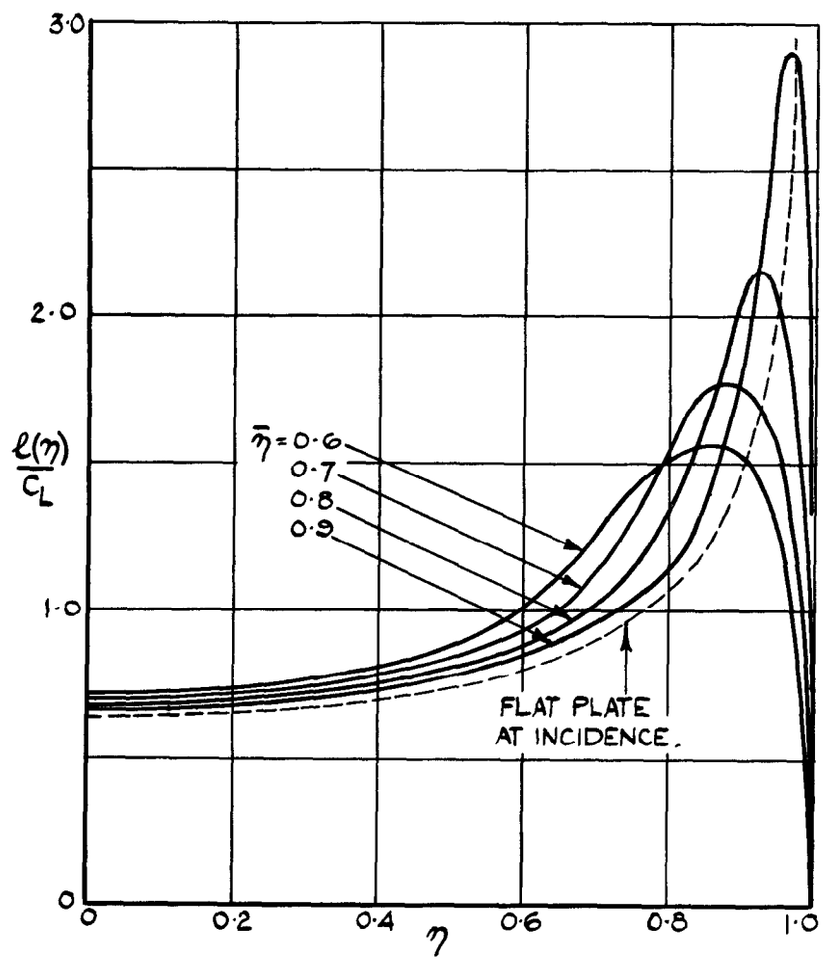

FIG.8. SPANWISE LOAD DISTRIBUTION.
$n = 2$.

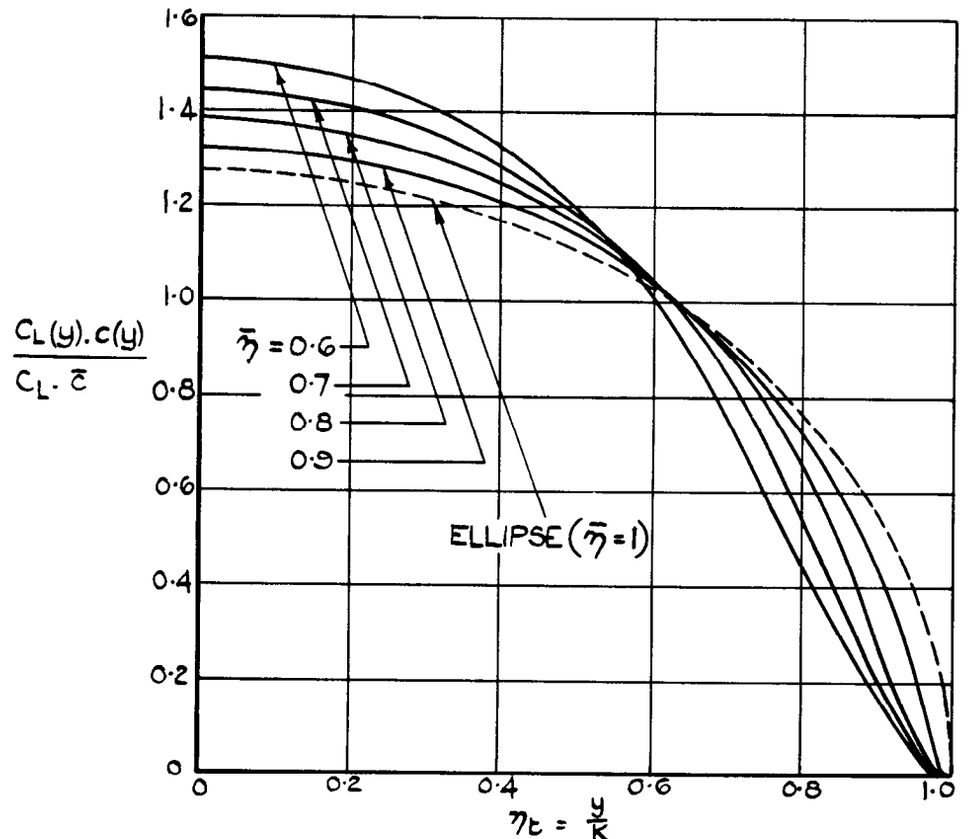

FIG.9. SPANWISE DISTRIBUTION OF CHORD LOAD.

$n = 1.$

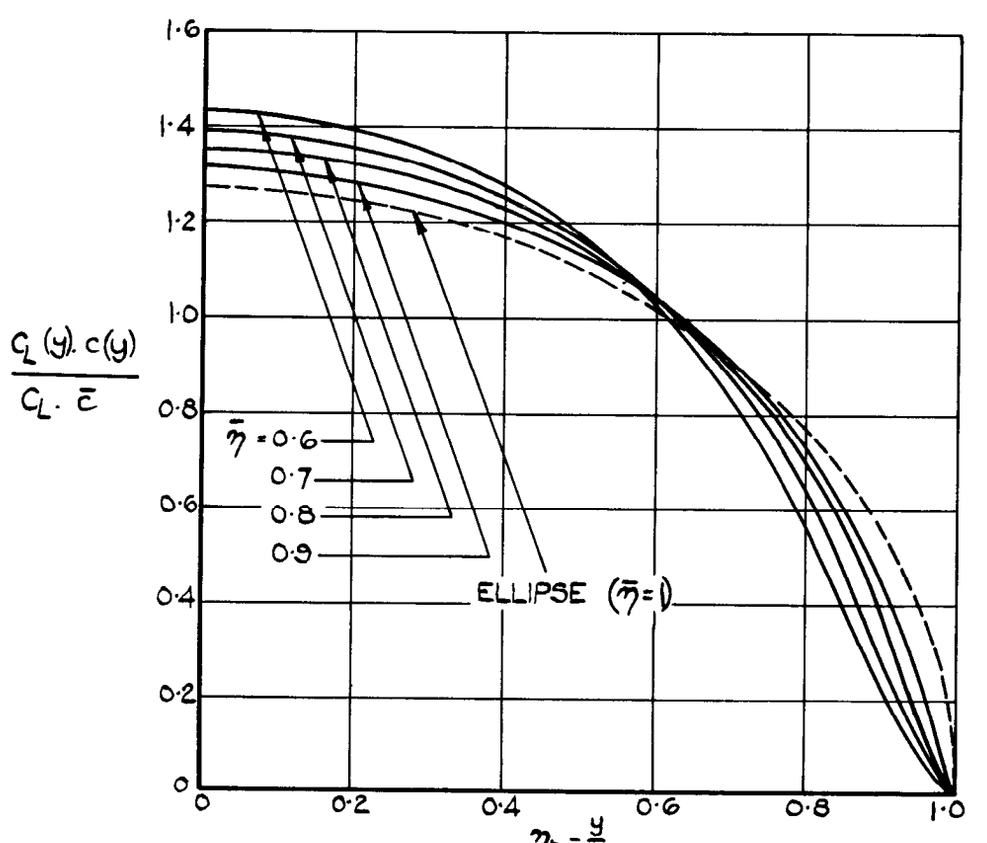

FIG.10. SPANWISE DISTRIBUTION OF CHORD LOAD.

$n = 2.$

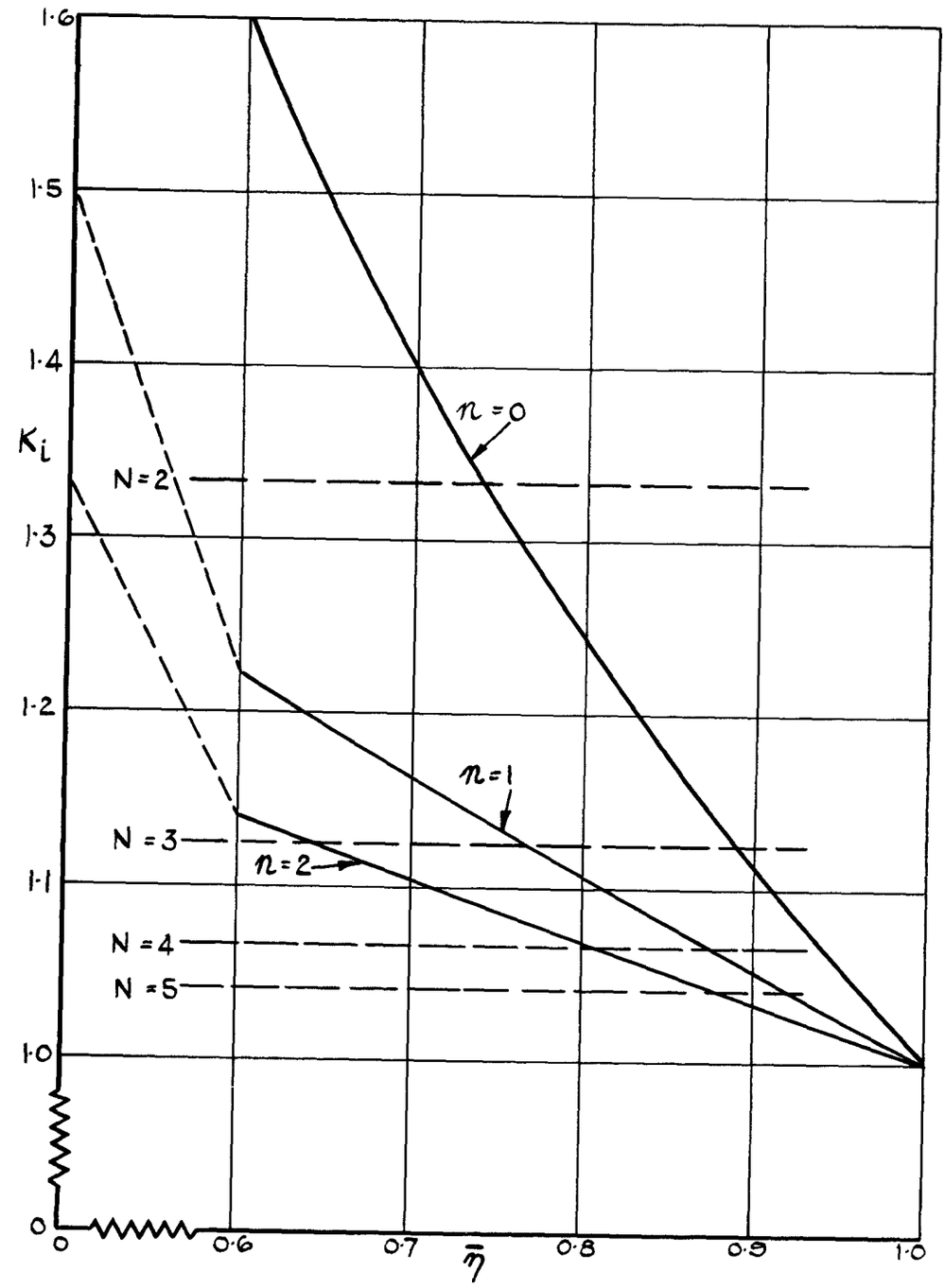

FIG.11. LIFT-DEPENDENT DRAG FACTOR, K_i.

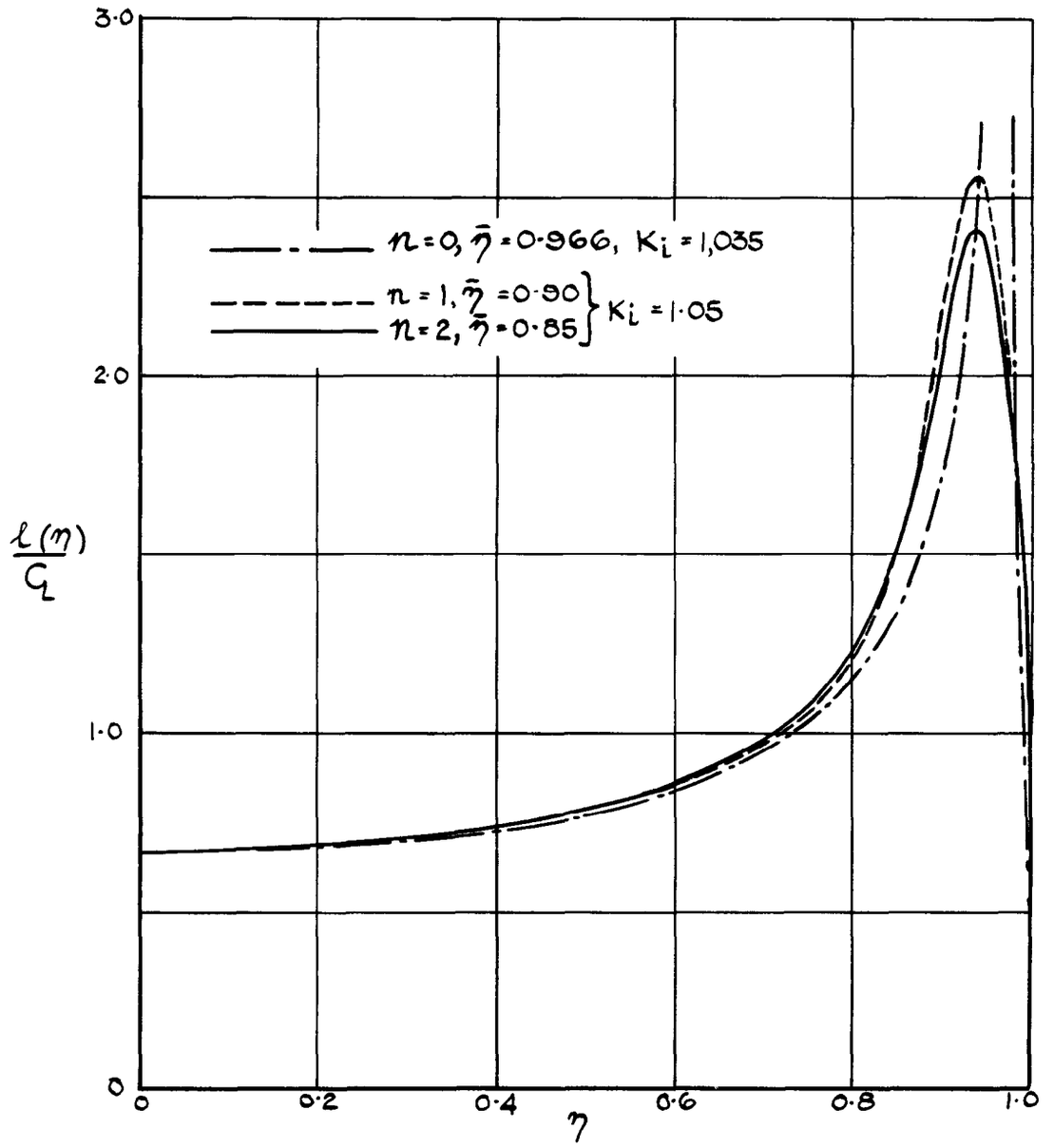

FIG.12. SPANWISE LOAD DISTRIBUTIONS FOR EQUAL VALUES FOR K_i.

C.P. No. 428
(19,957)
A.R.C. Technical Report

Published by
HER MAJESTY'S STATIONERY OFFICE

To be purchased from
York House, Kingsway, London W.C.2
423 Oxford Street, London W.1
13A Castle Street, Edinburgh 2
109 St. Mary Street, Cardiff
39 King Street, Manchester 2
Tower Lane, Bristol 1
2 Edmund Street, Birmingham 3
80 Chichester Street, Belfast
or through any bookseller

Printed in Great Britain

S.O. Code No. 23-9011-28

C.P. No. 428